17th AIAA International Space Planes and Hypersonic Systems and Technologies Conference
11 - 14 April 2011, San Francisco, California

AIAA 2011-2360

Plasma Control of an Unstarting Supersonic Flow

Seong-kyun Im[1], Hyungrok Do[2] and Mark A. Cappelli[3]
Mechanical Engineering Department, Stanford University, Stanford, California, 94305-3032

The control of unstart of a supersonic model inlet flow is demonstrated at Mach 4.7 flow conditions using a dielectric barrier discharge (DBD) actuator. Rayleigh scattering from condensed CO_2 particles is used to visualize flow features such as boundary layers and shock waves at low freestream static pressure (1kPa) and temperature (60K). Three inlet wall flow conditions - a laminar boundary layer, and a tripped turbulent boundary layer with and without plasma actuation, are tested for comparison in the measured time to unstart. The delay of the unstart process, initiated by mass addition to the supersonic flow, is demonstrated through the plasma actuation of the tripped freestream boundary layer when a single DBD actuator pair is oriented parallel to the freestream flow, generating spanwise disturbances. The effect of DBD actuation on this unstart process is limited to a region within about 3mm from the exposed electrode edge.

I. Introduction

UNSTART, a condition that can cause in-flight scramjet engine malfunction has been described by several researchers.[1-6] Unstart is believed to be caused by the thermal choking of the internal supersonic flow that results from the heat release in the combustor.[7-8] A rise in pressure following heat release in the inlet duct leads to boundary layer growth and separation. This cascades into disturbances and blockage of the upstream flow.[9] In ground test facilities, it is difficult to reproduce combustion-driven unstart as it requires a facility to provide high enthalpy supersonic flows for relatively long durations (e.g., seconds). The physics of the unstart process can be studied by at least partially reproducing flight condition, for example, flight Mach number and pressure but low temperature.[10] In the study described here, thermal choking is mimicked by mass injection into relatively cold Mach 4.7 freestream flow. We recently demonstrated[11-12] that the growth and separation of turbulent boundary layers strongly affect the unstart process. Boundary layer control in a scramjet inlet-duct can therefore provide extended engine performance and operating margins. There have been several studies of unstart transition delay through the use of isolators and boundary layer bleeding.[8] In this paper we present studies of dielectric barrier discharge (DBD) actuation of turbulent boundary layers in a supersonic flows and the associated use in controlling supersonic inlet-duct flows.

A dielectric barrier discharge (DBD) actuator typically consists of flow-exposed and dielectric embedded electrodes driven by alternating current (AC). An asymmetric configuration is designed to impose a force on the ionized gas generated by the discharge and to induce a directional flow of neutral gas through collisions with the drifting ions. Numerous studies have demonstrated effective subsonic flow control[13] through separated boundary layer re-attachment[14-17], boundary layer transition delay[18] and turbulent boundary layer manipulation.[19,20] The use of such DBD actuators have increased dramatically since their first introduction by Roth et al.[21] The research attention is now placed on efforts to understand the DBD actuation mechanism[22], including the interactions between actuator pairs[23], and to develop robust models and simulations of actuator performance[13]. Unlike the case of subsonic flow actuation, there have been only few studies[24] of low power DBD actuation for the control of supersonic flows. Most supersonic flow control studies that engage plasmas generally employ relatively high power direct current (DC) discharges[25-27]. Boundary layer control is a major issue in supersonic flow research, particularly with the resurgence in interest in the development of scramjet engines.

In our studies, important flow features (e.g. boundary layers, slip lines, shock waves, and shock-wave boundary-layer interactions (SWBLI)) are visualized by Planar Laser Rayleigh Scattering (PLRS) of a laser sheet from

[1] Graduate Student, AIAA Student Member.
[2] Post Doctoral Researcher, AIAA Student Member.
[3] Professor.

condensed CO_2 particles. This diagnostic technique was first proposed by Miles and colleagues[28-29] as a flow visualization method that is suitable in low temperature and low pressure supersonic flows expanded through the diverging section of converging/diverging nozzles. Gaseous CO_2 condensed by the sudden temperature drop during expansion and acceleration form nanometer-size particles which serve as markers of flow structure through scattered laser light. These CO_2 particles sublime in flow regions where the static temperature increases (e.g., within boundary layers or following strong shocks), and so the boundaries between these regions are discerned with high fidelity and contrast. This PLRS visualization enables us to observe these flow features under unstart flow conditions.

II. Experimental Setup

The experiment consists of a supersonic flow tunnel, a laser diagnostic system, and a longitudinal DBD actuator pair fabricated into the wall of a model inlet-duct in which air is injected through one wall, as shown schematically in Fig 1. A blow-down wind tunnel generated by a two-dimensional converging/diverging nozzle (25:1 area ratio) is used to produce the supersonic flow. The freestream Mach number (Ma = 4.7) of the base flow in the test section is determined by measuring the incident/reflected shock angle on a test wedge and is independently confirmed by PIV measurements. High pressure air and CO_2 mixtures (P_0 = 350 kPa and T_0 = 300 K, 3:1 volume ratio) expands into the 40 mm by 40 mm cross sectional area tunnel test section. The useful test time is approximately 5 seconds, limited by the pressure that can be maintained in the vacuum chamber. The static pressure and temperature of the flow in the test section during this time is approximately 1 kPa and 60 K, respectively. Optical access is provided by windows placed on both sides of test section. Static pressure traces on the bottom wall of the tunnel are recorded using a fast response pressure sensor (PCB Piezotronics, Model 113B26). This pressure trace will be used to determine the time to reach unstart after jet injection (discussed below).

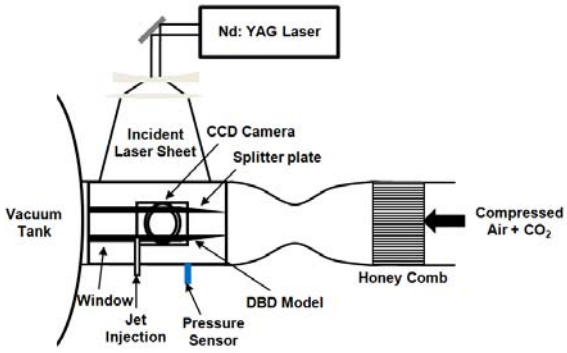

Figure 1. Schematic of experimental setup.

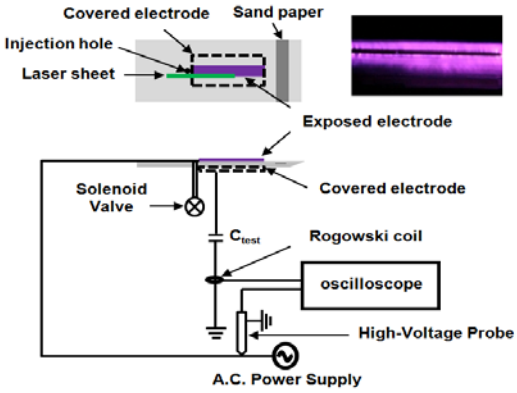

Figure 2. DBD actuator model.

The model inlet-duct is defined by two wedged flat plates (shown in Fig. 1) that span the 40 mm width of the tunnel. The upper wedged flat plate is fabricated from a polycarbonate plate to enable laser access into the inlet duct flow. A DBD actuator is integrated into the upper surface of the lower wedged flat plate. The portion that accommodates the DBD actuator was fabricated out of cast acrylic, with an epoxy (Loctite Hysol 1C) serving as a dielectric layer (approximately 2 mm thick) isolating the buried electrode from the top exposed electrode and discharge. Both electrodes consist of a single copper metal strip, oriented parallel to the flow (streamwise direction). The exposed and buried electrodes (0.1 mm thick) are 75 mm in length and 7 mm wide, and 75 mm in length and 25 mm wide, respectively. The exposed electrode is centered over the buried electrode, and both electrodes are placed along the center of the model with the leading edge of the electrodes located 40 mm downstream from the model leading edge. A 3 mm diameter hole is located at the end of the DBD actuator, 118 mm downstream of the leading edge, to introduce a sonic air jet. As shown in Fig. 2, the laser sheet (500 μm thickness) illuminates a region of interest. An AC power supply is used to drive the surface DBD discharge. A Rogowski coil (Pearson Electronics, Model 2877) and a 1000:1 high voltage probe (Tektronix, P6015A) are used to record current and voltage traces, respectively. The DBD actuator is driven at 20 kHz (with the buried electrode grounded), 6 kV peak to peak conditions. A typical image of its emission (viewed from above) while exposed to the Ma = 4.7 flow taken by a digital camera with 1/30 second exposure time is presented at the upper corner of Fig. 2.

A Nd:YAG laser (New wave, Gemini PIV, 100mJ/pulse energy, 10Hz, 532nm) is shaped into a thin sheet using two cylindrical lenses and a convex spherical lens, and is directed into the test section. A CCD camera (La Vision, Imager Intense) detects the scattered light at 90^{o} to the laser sheet. Laser firing for the PLRS is synchronized with the CCD camera exposure (3 μs). The laser signal triggers the jet injection during tunnel operation and is delayed as desired by a pulse delay generator (SRS, DG 535) to acquire images at different phases. The jet injection is controlled by a solenoid valve (ASCO, Red Hat II) driven by a controller (Optimal Engineering System Inc.), receiving its trigger signal from the delay generator. A sonic jet (air, 100 psi stagnation pressure and ambient stagnation temperature) is injected into the test section through the 3 mm diameter hole in the DBD model resulting in a flow disturbance and an overall increase in flow pressure and temperature.

Three flow configurations are studied, as shown in Fig. 3. Two wedged plates are used in all three configurations. With two plates, the inlet flow is fully isolated from the lower and upper wall turbulent boundary layer, but still experiences the thick (~ 1 cm) turbulent boundary layers on the side wall. In this study the height of the model flow is 15 mm. In the first configuration (Case I), boundary layers grow naturally from the leading edge of the each plate. For Case II and III, sand paper (120 Grit, 40 mm wide and 20 mm long) is attached to the top of the DBD model 10 mm downstream from the leading edge to trip the otherwise laminar boundary layer, creating a relatively thick turbulent boundary. The DBD actuator is only activated in the Case III flow configuration.

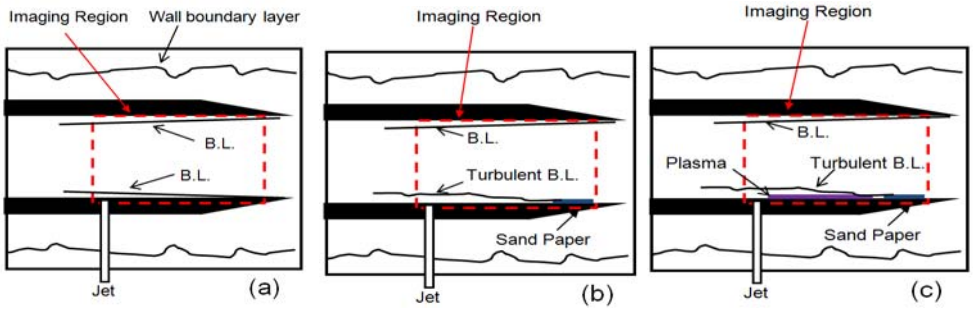

Figure 3. Schematic of flow configurations: (a) Case I, (b) Case II, (c) Case III.

III. Results

A. Flow visualization of three flow configurations

The time sequential images of Case I, II and III flow features while the flow undergoes unstart induced by the jet injection are illustrated in Figs. 4, 5 and 6, respectively. The images in Fig. 4, 5 and 6 are interrogated in two separate PLRS frames. The left frame illuminates the region in the vicinity of the jet and the right frame illuminates the upstream region near the wedge tip. (the flow is from right to left) All images in this section are taken with a laser sheet which is aligned with the edge of the exposed electrode. The approximate thickness (to within about 20%) of the boundary layer can be estimated by measuring the height of the dark region on the wall. [30]

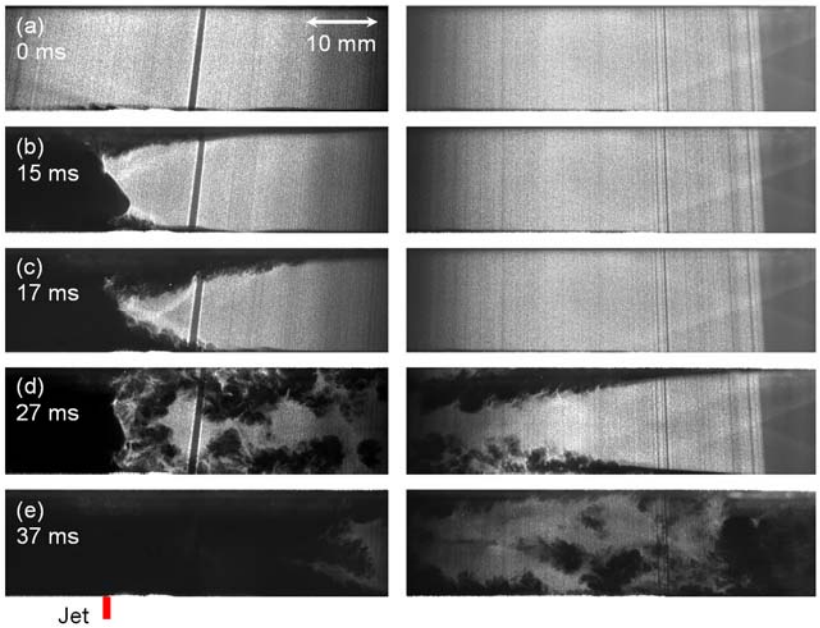

Figure 4. Time sequential PLRS images in the Case I flow configuration.

The unstart process for the Case I flow configuration is depicted in Fig. 4. The two wedged plates isolate the flow from thick upper and lower tunnel wall boundary layer. As a result, symmetric and thin laminar boundary layers on both upper and lower plates grow from the leading edge of the inlet walls, as shown in Fig. 4 (a). Shortly after jet injection (approximately 15ms, Fig. 4 (b)) separated boundary layers and oblique separation shockwaves on both plates are seen close to where the jet is injected and the flow field is abruptly disrupted. In Fig. 4 (c), boundary layer growth and separation ensues, and the propagation of these symmetric oblique shockwaves is apparent. These shocks eventually merge into pseudo-shocks which remain relatively stationary for some time (~10 ms) 60 mm upstream of the jet as depicted in Fig. 4 (d). The unstart that follows (Fig. 4(e)) is caused by the eventual break down of this pseudo-shock structure.

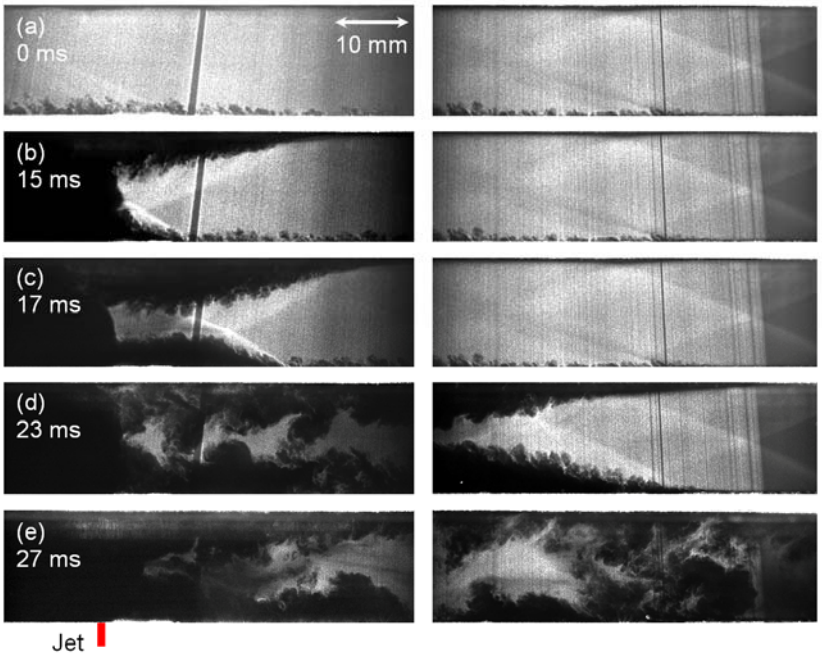

Figure 5. Time sequential PLRS images in the Case II flow configuration.

A similar illustration of this unstart process for the Case II flow configuration is presented in Fig. 5. Here we again have a laminar boundary layer condition on the upper wall, but there is a relatively thick turbulent boundary layer on the lower wall due to the the flow trip, as seen in Fig. 5 (a). The presence of the turbulent boundary layer leads to an asymmetric boundary layer condition. As a result, a relatively strong oblique shock wave forms on the turbulent boundary layer side following jet injection, and this shock propagates upstream as depicted in Fig. 5 (b) ~ (e). The pseudo-shock does not appear in this case. Unlike Case I, this oblique shockwave does not become quasi-stationary and so, the duration of unstart process for this configuration is much shorter than that of Case I.

The flow results for these cases described above are reproductions of conditions described by Do et al.[11,12] which confirm that the strong oblique unstart shock is formed on the turbulent boundary layer side and is independent of the side on which the jet is injected. The presence of a turbulent boundary layer is found to expedite the unstart process. It was argued in those studies that the delay of unstart with symmetric laminar boundary layers is due to the slow build-up of pressure behind the pseudo-shock. We believe that the unstart process can be delayed in the case of a turbulent boundary layer condition by appropriate actuation to produce an increase streamwise momentum flux within the boundary layer.

This unstart delay by DBD actuation is tested (Case III) under conditions of the Case II flow. The result of this actuation is described in Fig. 6. We can see (by comparison to Fig. (5)) that the thickness of the freestream boundary layer is significantly decreased and relaminarization is observed between the actuator tip and jet (Fig. 6 (a)). At the end of the actuator, this laminarization is quickly lost and the boundary layer returns to its turbulent state. In Fig. 6 (b) and (c), the effect of this transition can be seen in the early stage of the unstart process as the appearance of relatively strong oblique unstart shockwaves on the DBD actuator plate. However, once the unstart shock reaches the controlled region, the structure of the shockwave appears to better resemble the pseudo-shock structure seen in the case of the symmetric laminar boundary layer conditions (Case I). This pseudo-shock remains quasi-stationary at a location of 70 mm upstream of the jet for approximately 2 ms, as indicated in Fig. 6 (d). While this quasi-stationary period is not quite as long as that of Case I, it is nevertheless apparent that the unstart process is controlled by this transition from an oblique shock to a standing pseudo-shock. Eventually, the increase in pressure behind this pseudo-shock leads to a breakdown in the structure, followed by flow disgorgement as depicted in Fig. 6 (e).

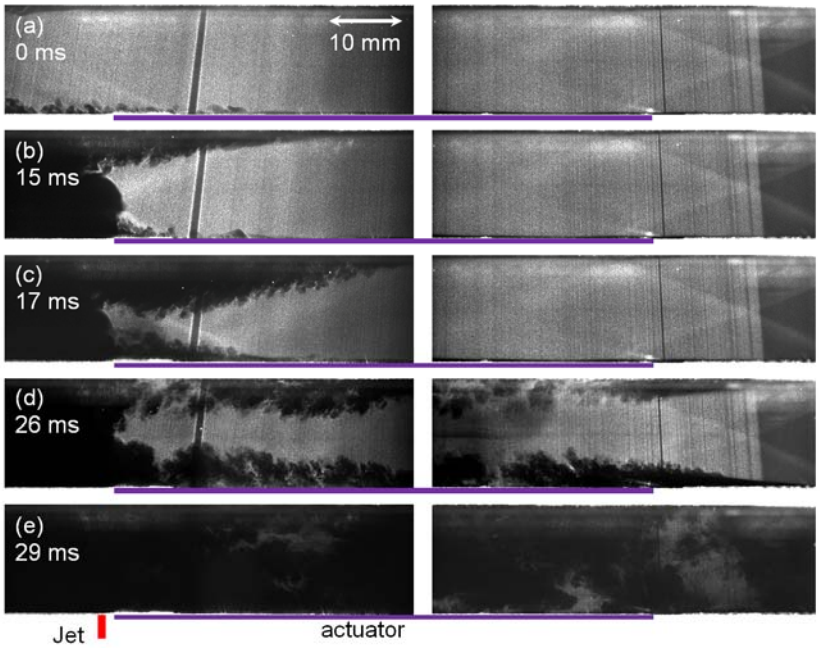

Figure 6. Time sequential Rayleigh scattering images in Case III flow configuration

B. Duration of unstart process

Several unstart runs were carried out to generate some statistics on the reduction in the unstart delay generated by this DBD plasma actuation. A quantitative marker for unstart time following jet injection is obtained from the rise in pressure a measured by the pressure sensor located on the lower wind tunnel wall (see Fig. (7)). Figs. 7 (a) and (b) are schematics that qualitatively represent flow conditions outside of the model inlet before and after unstart, respectively. Before unstart, the flow is relatively undisturbed and the pressure sensor signal (represented as a blue line in Fig. 7 (c)) is relatively steady and stable. However, once the unstart shock propagates beyond the model inlet, the tunnel flow is strongly disturbed and a rapid increase in wall pressure is detected by the arrival of a strong (presumably normal) shock. The unstart time, which is defined here as the time, between jet trigger signal and rise in pressure at the location of this sensor can be determined quite accurately, as seen in Fig. 7 (c).

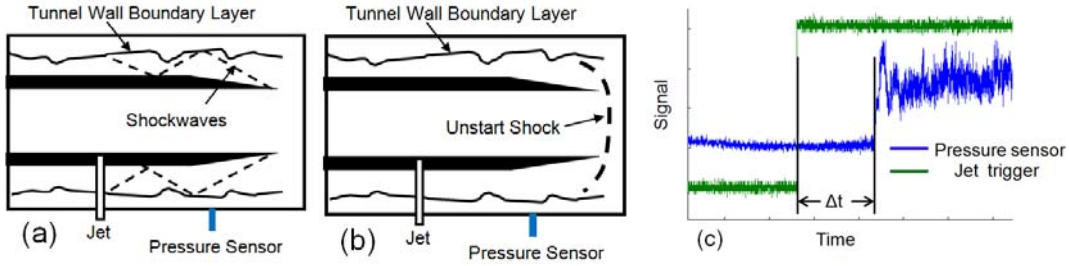

Figure 7. Schematic of flow condition (a) before unstart, (b) after unstart, and (c) pressure signal and jet trigger signal

Fifty experiments were carried out for each of the three flow configurations (Cases I – III), generating preliminary statistical data as described in Fig. 8. The histograms (and the superimposed t-distribution fits) represent probability density functions that describe the unstart time. The blue, green and red color illustrate the results for Case I, II and III, respectively. The averaged unstart time for Case I, II and III is 38.4 msec, 27.9 msec and 29.6 msec, respectively. The discrepancy between Case I and II is 10.5 ms and is due to the different shock structures seen, as discussed above. With the DBD actuation, the unstart process is delayed by about 1.7 msec, i.e., by about 16% the difference in unstart time between Cases I and II, which serves as a benchmark. It is clear that the actuation is not sufficiently robust at this time to generate unstart flow conditions comparable to those of Case I (laminar boundary layers). Improvements must be made to the actuator configurations to improve actuator performance. To do so, we describe below initial characterization of the detailed flow within the region of the actuators.

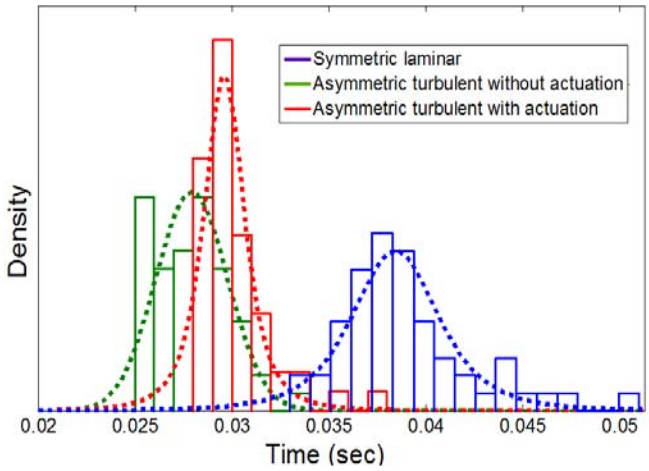

Figure 8. Histgram of unstart duration and t-distribution fitting

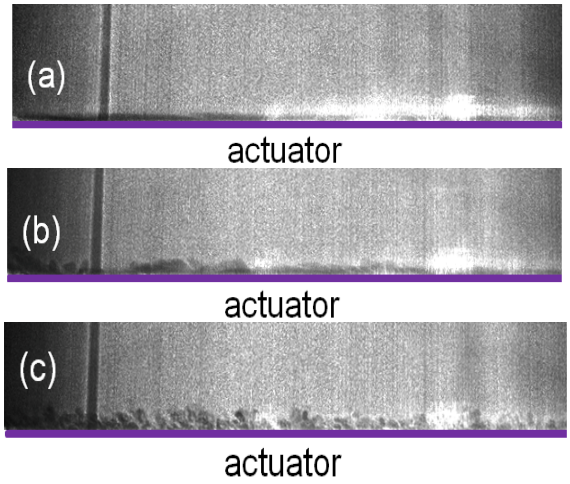

Figure 9. PLRS images of laser sheet intersecting the plane crossing (a) exposed electrode edge, (b) 1.5 mm from the edge, and (c) 3 mm from the edge.

We believe that the actuation occurs as a result of the downward flow induced by the DBD, that carried high momentum fluid into the boundary layer. This downward jet is expected to be strongest near the edge of the exposed electrode. Under flow conditions of Case III (with DBD actuation), the laser sheet location is moved to sample the flow at various spanwise distances away from the edge of the exposed electrode. Fig. 9 (a), (b) and (c) depict PLRS images of the exposed electrode edge, 1.5 mm from the edge, and 3 mm from the edge, respectively. It is apparent that a relaminarization of the boundary layer occurs in Fig. 9 (a). However, the diminishing of this relaminarization, as seen in Fig. 9 (b), and Fig. 9 (c), implies that this relaminarization is confined to a relatively small region of the flow, in the vicinity of the actuator edge (within about 3 mm). We believe that we can enhance the effectiveness of this DBD actuation for unstart delay by increasing this actuation area. Future studies will include the use of multiple electrodes in the DBD design to access a greater volume of the free stream flow.

IV. Conclusion

In this paper, we examine the use of dielectric barrier discharge actuators as a possible method of controlling mass injection-induced unstart in a model supersonic inlet flow. Flow features are visualized by Planar Laser Rayleigh Scattering off of condensed CO_2 particles. Three inlet model flow configurations, all of which use two wedged plates to isolate the flow from thick upper and lower turbulent tunnel wall boundary layers, were investigated (Cases I-III). In the Case I flow configuration, the upper and lower wall of the inlet flow have symmetric laminar boundary layers that grow naturally from tip of the plates. For this configuration, a pseudo-shock structure that is stationary for about 10 msec is observed to form during the unstart process. In the Case II flow configuration, an asymmetric boundary layer condition is established, with a tripped boundary layer on the DBD actuator side. Here, a pseudo-shock does not appear and instead, a strong oblique unstart shock dominates the dynamics of this unstart. Partial control of this unstart seen in Case II is demonstrated by DBD actuation on the tripped boundary layer (Case III). The actuation results in a suction-like plasma response, which draws high momentum fluid from the core into the turbulent boundary layer. PLRS images suggests that a local re-laminarization occurs, and with that, the shock structure appears more of a resemblance to the pseudo-shock structure seen for Case I. This pseudo-shock is also quasi-steady (but its lifetime is shorter than that of Case I). Preliminary statistical studies are conducted to quantify the unstart margin for these three cases, by defining the

unstart time as the time relative to the triggering of the jet, for a pressure disturbance to be detected outside of the inlet flow, along the lower tunnel wall. This unstart time for Case II is reduced by about 2 ms by the application of the discharge, suggesting that in its present configuration, this actuator is weakly effective. The effective suction is found to be highly localized (to the vicinity of the edge of the upper electrode), and future experiments will examine the possible increase in the robustness of this unstart control by distributing multiple actuators across the spanwise direction of the inlet flow.

Acknowledgments

This research is performed through the Stanford Predictive Science Academic Alliance Program (PSAAP) Center, supported by the Department of Energy (National Nuclear Security Administration) under Award Number DE-FC52-08NA28614.

References

[1]Emami S., Trexler C. A., Auslender A. H., and Weidner J. P., "Experimental investigation of inlet-combustor isolators for a dual-mode scramjet at a Mach number of 4," NASA Technical Paper 3502, 1995.

[2]Wieting A. R., "Exploratory study of transient unstart phenomena in a three-dimensional fixed-geometry scramjet engine," NASA TN D-8156, 1976.

[3]Rodi P. E., Emami S., and Trexler C. A., "Unsteady Pressure Behavior in a Ramjet/scramjet Inlet," *Journal of Propulsion and Pow*er, Vol. 12, No. 3, 1996, pp. 486-493.

[4]Shimura T., Mitani T., Sakuranaka N., and Izumikawa M., "Load Oscillations Caused by Unstart of Hypersonic Wind Tunnels and Engines," *Journal of Propulsion and Power*, Vol. 14, No. 3, 1998, pp. 348-353.

[5]O'Byrne S., Doolan M., Olsen S. R., and Houwing A. F. P., "Analysis of Transient Thermal Choking Processes in a Model Scramjet Engine," Journal of Propulsion and Power, Vol. 16, No. 5, 2000, pp. 808-814.

[6]Graham R. H., *SR-71 Blackbird*, MBI Publishing Company, St. Paul, MN, 2002, pp. 27-28.

[7]Mashio, S., Kurashina, K., Bamba, T., Okimoto, S., and Kaji, S., "Unstart Phenomenon Due to Thermal Choke in Scramjet Module," *AIAA/NAL-NASDA-ISAS 10th International Space Planes and Hypersonic Systems and Technologies Conference*, 2001, AIAA 2001-1887.

[8]Kodera, M., Tomioka, S., Kanda, T., Mitani, T., and Kobayashi, K. "Mach 6 Test of a Scramjet Engine with Boundary-Layer Bleeding and Two-Staged Fuel Injection," *12th AIAA International Space Planes and Hypersonic Systems and Technologies*, 2003, AIAA 2003-7049.

[9]McDaniel K. S. and Edwards J. R., "Three-Dimensional Simulation of Thermal Choking in a Model Scramjet Combustor," *39th Aerospace Sciences Meeting and Exhibit*, 2001, AIAA 2001-0382.

[10]Wagner J. L., Yuceil K. B., Valdivia A., Clemens N. T., and Dolling D. S., "Experimental Investigation of Unstart in an Inlet/isolator Model in Mach 5 Flow,"AIAA Journal, Vol. 47, No. 6, 2009, pp. 1528-1542.

[11]Do, H., Im, S. Mungal, M. G., and Cappelli, M. A., "Visualizing Supersonic Inlet Duct Unstart Induced by Jet Injection using Rayleigh Scattering from Condensed CO_2," *Experiments in Fluids*, 2010. (published online)

[12]Do, H., Im, S. Mungal, M. G., and Cappelli, M. A., "The Influence of Boundary Layers on Supersonic Inlet Flow Unstart Induced by Mass Injection," *Experiments in Fluids*, 2010. (accepted to be published)

[13]Moreau, E., "Airflow Control by Non-Thermal Plasma Actuators," *Journal of Physics D: Applied Physics*, Vol. 40, No. 3, 2007, pp. 605-636.

[14]Do, H., Kim, W., Mungal, M. G., and Cappelli, M.A., "Bluff Body Flow Separation Control using Surface Dielectric Barrier Discharges," *45th AIAA Aerospace Sciences Meeting and Exhibit*, 2007, AIAA 2007-939.

[15]Post, M. L., and Corke, T. C., "Separation Control on High Angloe of Attack Airfoil Using Plasma Actuators," *AIAA Journal*. Vol.42, No. 11, 2004, pp. 2177-2184.

[16]Huang, J., Corke, T. C., and Thomas, F. O., "Unsteady Plasma Actuators for Separation Control of Low-Pressure Turbine Blades," *AIAA Journal*. Vol. 44, No. 7, 2006, pp. 1477-1487.

[17]Sung, Y., Kim,W., Mungal, M. G., and Cappelli, M. A., "Aerodynamic Modification of Flow Over Bluff Objects by Plasma Actuation," *Experiments in Fluids*, Vol. 42, No. 3, 2006, pp. 479-486.

[18]Grundmann, S., and Tropea, C., "Experimental Transition Delay Using Glow-Discharge Plasma Actuators," *Experiments in Fluids*, Vol. 42, No. 4, 2007, pp. 653-657.

[19]Porter, C. O., Baughn, J. W., McLaughlin, T. E., Enloe, C. L., and Font, G. I., "Plasma Actuator Force Measurements," *AIAA Journal*. Vol. 45, No. 7, 2007, pp. 1562-1570.

[20]Schatzman, D. M., and Thomas, F. O., "Turbulent Boundary Layer Separation Control Using Plasma Actuators," *4th Flow Control Conference*, 2008, AIAA 2008-4199.

[21]Roth, J. R., Sherman, D. M., and Wilkinson, S. P., "Boundary Layer Flow Control with a One Atmosphere Uniform Glow Discharge Surface Plasma," *36th AIAA Sciences Meeting and Exhibit*, 1998, AIAA 1998-0328.

[22]Kim, W., Do, H., Mungal, M. G., and Cappelli, M. A., "On the Role of Oxygen in Dielectric Barrier Discharge Actuation of Aerodynamic Flows," Applied Physics Letters, Vol. 91, 2007, pp. 181501.

[23]Do, H., Kim, W., Cappelli, M. A., and Mungal, M. G., "Cross-talk in Multiple Dielectric Barrier Discharge Actuators," Applied Physics Letters, Vol. 98, 2008, pp. 071504.
[24]Im, S., Do, H., and Cappelli, M. A., "Dielectric Barrier Discharge Control of a Turbulent Boundary Layer in a Supersonic Flow," Applied Physics Letters, Vol. 97, 2010, pp. 041503.
[25]Leonov, S., Bityurin, V., Savischenko, N., Yuriev, A., and Gromov, V., "Influence of Surface Electrical Discharge on Friction of Plate in Subsonic and Transonic Airflow," *39th AIAA Aerospace Sciences Meeting and Exhibit*, 2001, AIAA 2001-640.
[26]Narayanaswamy, V., Raja, L. L., and Clemens, N. T., "Characterization of a High-Frequency Pulsed-Plasma Jet Actuator for Supersonic Flow Control," *AIAA Journal*. Vol. 48, No. 2, 2010, pp. 297-305.
[27]Menier, E., Leger, L., Depussay, E., Lago, V., and Artana, G., "Effect of a DC Discharge on the Supersonic Rarefied Air Flow Over a Flat Plate," Journal of Physics D: Applied Physic, Vol. 40, No. 3, 2007, pp. 695-701.
[28]Miles, R. B., and Lempert, W. R., "Quantitative flow visualization in unseeded flows," *Annual Review of Fluid Mechanics*, Vol. 29, 1997, pp. 285-326.
[29]Wu, P., Lempert, W. R., and Miles, R. B., "Megahertz Pulse-Burst Laser and Visualization of Shock-Wave/Boundary-Layer Interaction," *AIAA Journal*, Vol. 38, No. 4, 2000, pp. 672 – 679.
[30]Poggie, J., Erbland, P. J., Smits, A. J., and Miles, R. B.,"Quantitative Visualization of Compressible Turbulent Shear Flows Using Condensate-Enhanced Rayleigh Scattering," *Experiments in Fluids*, Vol. 37, No. 3, 2004, pp. 438-454.